

DETERMINATION OF INFLOW PERFORMANCE RELATIONSHIP FOR A VERTICAL WELL IN NATURALLY FRACTURED OIL RESERVOIRS: NUMERICAL SIMULATION STUDY

Reda Abdel Azim, Melissa Ramirez, and Mohammad R, Awal

American University of Ras Al Khaimah, United Arab Emirates, Ras Al Khaimah

Received December 24, 2017; Accepted March 19, 2018

Abstract

The Inflow Performance Relationship (IPR) of a well is a relation between the oil or gas production rate and the flowing bottom-hole pressure. This relationship serves as an important tool for petroleum engineers to understand and predict well performance. The IPR correlations are used to design and evaluate well completion, optimize well production, and design artificial lift method. There are several IPR correlations reported in the literature, mostly for homogeneous and isotropic reservoirs.

For naturally fractured reservoirs (NFR), which account for almost half of the world's remaining oil reserves, the challenge of predicting reservoir as well as well flow performances is daunting due to the heterogeneous flow in the complex fracture networks. Recently some IPR correlations have been reported for both naturally and hydraulically fractured reservoirs using analytical methods. However, the analytical methods do not represent the complex fractures networks in the NFRs, and the best practice has been, for addressing reservoir flow performance, numerical reservoir simulation approach to model the complex fracture networks as well as model the relative permeability functions of the flowing fluid phases.

In this work, therefore, numerical reservoir simulation approach is adopted in order to develop a new IPR model for oil wells in a NFR. The new model is semi-analytical: first, a 3D black-oil reservoir simulator developed by the lead author is used to develop the oil mobility function (OMF) that captures the complex fluid flow in the fracture networks; then the OMF is used to analytically compute the IPR function. The simulation runs are set up with data from well test analysis along with permeability and pressure-volume-temperature data in the fluid flow equations. In the numerical simulation runs, four different oil flow rates are used to generate the oil saturation and corresponding relative permeability in the naturally fractured reservoir. Comparisons between the new method and two popular correlations for non-fractured reservoirs indicate the necessity for developing and using an IPR correlation specifically developed for a fractured reservoir.

Keywords: *inflow performance relationship; mobility function; naturally fractured reservoir; well test analysis.*

1. Introduction

The Inflow Performance Relationship (IPR) of a well is a non-linear equation between the oil or gas volumetric production rate (q_o or q_g) and the flowing bottom-hole pressure (p_{wf}) that represents the reservoir pressure at the well-reservoir interface. IPR analysis is used to develop optimum reservoir flow rate and flowing bottom hole reservoir pressure for oil and gas wells in various types of reservoir systems, especially during the prolonged pseudo steady-state flow period. The relationship can be derived from the classical diffusivity equation, as originally developed by Muskat and Evinger [1] attempted to account for the observed nonlinear flow relationship (q_o vs p_{wf}) during the pseudo steady-state flow of oil as follows:

$$q_o = \frac{kh}{141.2 \left[\ln \left(\frac{r_e}{r_w} \right) - 0.75 + s \right]} \int_{p_{wf}}^{p_R} \frac{k_{ro}}{\mu_o B_o} dp \quad (1)$$

Equation (1) is valid for a homogeneous and isotropic reservoir, for radial flow in a circular reservoir with a fully penetrating vertical well at the center. The integrand is defined as the

transmissibility function, $T_f(k_{ro}, \mu_o, B_o)$, which is a function of oil-phase saturation (s_o), and the pressure-dependent oil PVT properties (μ_o, B_o):

$$T_f(k_{ro}, \mu_o, B_o) = \frac{k_{ro}}{\mu_o B_o}$$

Given that reservoir pressure changes with time, coupled with obtaining a single permeability value to represent the entire reservoir domain, and the relative permeability term being dependent on oil saturation (s_o) which vary with time and from the drainage boundary to the wellbore, Equation (1) is anything but practical for practicing production engineers in order to predict well productivity as a function of time.

To circumvent the problem, Vogel [2] introduced an easy-to-use method for predicting the performance of a vertical oil well producing oil and associated gas from a solution-gas drive reservoirs. His empirical inflow performance relationship (IPR) is based on computer simulation results and is given by. The correlation between dimensionless pressure, $\left(\frac{p_{wf}}{P_r}\right)$, and dimensionless oil flow rate, $\left(\frac{q}{q_{max}}\right)$, was found to be valid for a range of common rock and fluid properties:

$$\frac{q}{q_{max}} = 1 - b \left(\frac{p_{wf}}{P_r}\right) - (1 - b) \left(\frac{p_{wf}}{P_r}\right)^2 \quad (2)$$

where, $b = 0.2$. The unknown parameter, q_{max} , is specific for a given reservoir, and encapsulates the effects of such flow conditions as formation damage or stimulation (negative, or positive skin effect, respectively), and needs to be estimated by conducting a stabilized production flow test.

It is to be noted that the purpose of using a numerical reservoir simulator (NRS) by these authors was to develop a large data set for production rate (q) and corresponding flowing bottomhole pressure (FBHP, p_{wf}) in the well, which overcomes the practical problem of obtaining representative FBHP along with oil flow rates without the effect of wellbore damage, hydraulic fracturing stimulation, well inclination, etc. Fetkovich [3] used well test data (Isochronal test method) to correlate FBHP with oil flow rate, which can also be rearranged in terms of Vogel's dimensionless variables, and the resulting empirical IPR model, which introduces a second parameter, n (flow exponent), and therefore, requires two well test data at different flow rates:

$$\frac{q}{q_{max}} = \left[1 - \left(\frac{p_{wf}}{P_r}\right)\right]^n \quad (3)$$

Several researchers extended Vogel's work to develop reservoir simulation-based empirical IPR models for homogenous, solution-gas drive reservoirs, in order to include such cases as well inclination, flow of water and solids, etc. For example, Cheng [4] employed Vogel's NRS technique to develop the IPR equation for a horizontal well:

$$\frac{q}{q_{max}} = 1 + 0.2055 \left(\frac{p_{wf}}{P_r}\right) - 1.1818 \left(\frac{p_{wf}}{P_r}\right)^2 \quad (4)$$

Wiggins [5] extended the work of Vogel [2] to include flow of reservoir and solid particles in the flow rate variable, q :

$$\frac{q}{q_{max}} = 1 - 0.52 \left(\frac{p_{wf}}{P_r}\right) - 0.48 \left(\frac{p_{wf}}{P_r}\right)^2 \quad (5)$$

Interested readers may find in Elias *et al.* [6] and Shahri *et al.* [7] a summary of various Vogel-type IPRs.

The Vogel-type IPR correlations are, are valid for isotropic and homogenous reservoirs. These are not valid for naturally fractured reservoirs, where fluid flow path is more complex due to matrix as well as fracture flow. As much as half of the remaining oil reserves in the world is located in NFRs, especially the carbonate reservoirs, and sometimes in igneous basement rocks [8]. The fracture networks provide a higher permeability flow path than the interconnected pores in the matrix. Therefore, using the Vogel-type IPR correlations would under-predict a well's production potential and performance. Only recently this problem was addressed, e.g., Jahanbani & Shadzadeh [9], who presented an analytical IPR model for a

naturally fractured, solution-gas drive reservoir. They used the well-known equation (1), in which the relative permeability term, k_{ro} , is obtained from laboratory measured values using a core obtained from the NFR under consideration. However, it is a common knowledge that a NFR is quite heterogeneous in respect of fracture characteristics, from fracture dimensions, and distribution over the flow domain. Therefore, a limited, lab-based relative permeability function, as used by Jahanbani & Shadizadeh [91], may not be representative of flow characteristics from reservoir outer boundary to the inner boundary (*i.e.*, the wellbore) in a NFR. Therefore, we adopt numerical reservoir simulation approach to evaluate the integral function in equation (1).

2. The new semi-analytical IPR model

In a saturated NFR, a matrix block is saturated with oil and partially by gas, where capillary pressure plays a significant role in oil recovery process.

Therefore, the design objective was to construct a reservoir flow model based on a commercial simulator to generate flow data as a function of pressure. Using the simulation generated data, we develop a correlation between oil mobility and average reservoir pressure. The oil mobility function is a key variable in the IPR equation.

The pseudo-steady state flow in a cylindrical naturally fractured reservoir (NFR) with a vertical well at the center of the drainage area is represented by the following equation.

$$p_{wf} = p_R - \frac{141.2 qB}{T_f} \left[\ln \left(\frac{r_e}{r_w} \right) + s - 0.75 \right] \quad (6)$$

$$\text{where, } T_f = \frac{162.6 qB}{m} = \frac{k_f h}{\mu} \quad m = \frac{162.6 qB}{T_f}$$

T_f (Fracture transmissibility) is calculated from the slope, m , of two parallel lines of the in a semi-log plot of pressure versus logarithm of time (data from transient test: drawdown and buildup tests from a well producing in a finite, naturally fractured reservoirs). Various equations and type curves have been presented in the literature to analyze such transient flow and pressure buildup tests.

When two-phase flow conditions prevail, Eq. (1) for oil phase flow can be approximated, by evaluating the fluid properties μ_o and B_o and relative permeability k_{ro} are evaluated at the average reservoir pressure, $p_{av} = \frac{p_{wf} + p_R}{2}$, as,

$$p_{wf} = p_R - \frac{141.2 q_o B_o}{T_f} \left[\ln \left(\frac{r_e}{r_w} \right) + s - 0.75 \right] \quad (7)$$

Substituting for T_f into the above equation gives, we obtain oil flow rate as follows:

$$q_o = \frac{0.00708 k_f h (p_r - p_{wf})}{\left[\ln \left(\frac{r_e}{r_w} \right) + s - 0.75 \right]} \left(\frac{k_{rf,o}}{\mu_o B_o} \right) p_{av} \quad (8)$$

In case of our studied reservoir, the drainage boundary is a square and not circular. Eq (8) is therefore adjusted to incorporate the reservoir shape factor, C_A , as follow:

$$q_o = \frac{0.00708 k_f h (p_r - p_{wf})}{\left[\frac{1}{2} \ln \left(\frac{4A}{\gamma C_A r_w^2} \right) + s \right]} \left(\frac{k_{rf,o}}{\mu_o B_o} \right) p_{av} \quad (9)$$

where: γ = Euler's constant = 1.78; A = drainage area; C_A = reservoir shape factor = 30.9 for square drainage boundary.

The objective now is how to find relationship between the mobility function, T_f , and the average reservoir pressure, p_{av} , as a function of time, in order to evaluate at a specific point of time the oil production rate from a vertical well at the center of a naturally fractured reservoir (NFR) of constant thickness and rectangular drainage boundary. The first step is to evaluate the permeability value, k_f , that represent the combined effect of matrix and fracture channel permeability for a given fracture aperture and distribution. Toward that end, we construct a 3D reservoir simulation model, which contains fracture map and permeability tensor. The workflow is described in detail by Abdelazim and Rahman [10], and Abdelazim [11]; therefore we present only an outline of the methodology here.

3. Generation of subsurface network fracture map

Fracture data analysis is the first step in reservoir characterization process. The analysis consists of the determination of types of fractures or fracture parameters that control the distribution and quality of flow zones. Borehole images and production data are used to identify a set of variables such as dip, azimuth, aperture, or density that controlling hydrocarbon flow. Fracture indicators such as production rates are combined with borehole images to flag the flow contributing fracture zones. This technique has been used successfully in fractured basement reservoirs [12-13]. The fracture sets are defined based on fractures dip, length, and azimuth. The initial data of fractures length and dip angles ranging from 9 m to 60 m and 70° to 90° respectively and the fracture aperture ranges from 0.004 mm to 0.04 mm. Once the fracture set has been identified, it is used in the form of a fracture intensity curve.

For flow simulation in the NFR, we divide the rectangular reservoir flow domain in to number of grid blocks. We use a hybrid methodology to simulate fluid flow, combining the single continuum and the discrete fracture approach. The 3D discrete fracture network is created that consists of two sets of fractures: (i) small to medium fractures (length < 40 m), and (ii) long fractures (length > 40 m), along with their density, orientations and locations. These fractures are considered as part of the matrix (in the form of *permeability tensor*, which can be contributing to local vertical heterogeneity).

Fracture intensity map is extracted from geological interpretations of reservoirs. Fractures are distributed stochastically with different radius, dip and azimuth angles using fracture intensity value of 0.1 m⁻¹. The fracture intensity is calculated by dividing the studied reservoir (500m x 500m x 30m) into different grid blocks and fractures that cut each block are well-defined. Fracture intensity is expressed as:

$$Fracture\ intensity = \frac{\sum_{i=1}^N Area}{Volume} \tag{10}$$

where, N is the total number of fractures that intersect the corresponding grid block.

The grid block along with small and medium fractures uses tetrahedral elements in 3D domain for matrix and triangular elements in 2D domain for fractures. Once the block-based permeability tensors (3D) are calculated, the reservoir domain along with long fractures are discretized by tetrahedral elements for matrix as well as triangular elements for fractures.

A threshold value for fracture length is defined by trial and error. The threshold length is selected depends on the effect of different fracture length on the reservoir performance. Fractures with length smaller than the threshold value are used to generate the grid-based *permeability tensor* in 3D, while fractures with length longer than the threshold value are explicitly discretized in the domain by using tetrahedral elements.

4. Estimation of block-based permeability tensor

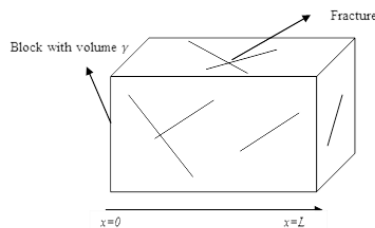


Figure 1. 3D cube used for permeability tensor calculations

In order to calculate the effective permeability tensors which represents an average permeability for the two structures, 3D cube is used to represent the matrix and fractures porous media (Fig.1).

The fractured porous media is bounded in an impermeable cover with boundary conditions for pressures (P₁ and P₂).

The boundary conditions are:

$$p(x = 0) = p_1, p(x = L) = p_2, J_n = 0 \text{ and } v = 0 \text{ on } s_1$$

The seepage velocity calculated based on the flow rate integration over fracture surfaces and matrix porous media and by using total volume of the block.

$$v = -\frac{k_m}{\mu} \nabla p \tag{11}$$

where μ the fluid viscosity and p is the pressure and the continuity equation for local seepage velocity in the matrix read as:

$$\nabla \cdot v = 0 \quad (12)$$

The hydraulic properties of fracture can be characterized by fracture transmissivity (aperture) and main flow rate is set parallel and normal to fracture plane. The flow rate J in fractures is usually defined by unit width of fracture and can be expressed by:

$$J = -\frac{k_{eff}}{\mu} \nabla_s p \quad (13)$$

In case of the flow is parallel to fracture plane, the seepage velocity normal to the fracture induces a pressure drop expressed by:

$$v = -\frac{1}{\mu} \nabla p \quad (14)$$

The effective fracture permeability of fracture can be describing by its aperture b as (in case the fractures are empty):

$$k_{eff} = -\frac{b^3}{12} \quad (15)$$

The mass conservation equation for the flow in a fracture is:

$$\nabla_s \cdot J = -\left(\vec{v}^+ + -\vec{v}^-\right) \cdot n \quad (16)$$

where n the unit vector is normal to fracture plane, \vec{v}^+ is the seepage velocity in the matrix on the side of n and \vec{v}^- is the seepage velocity on the opposite side.

This transport equation is implemented with the above-mentioned boundary conditions to calculate the permeability tensors.

Therefore, the total seepage velocity over the block is obtained by integrating the flow rates over fracture surfaces and matrix porous media. Then the results divided by the total block volume to calculate the block effective permeability tensor.

$$v_x = \frac{1}{\gamma} \left\{ \int_{\gamma m}^- v_x dv + \int_{sf}^- J_x ds \right\} = \frac{-k_{eff}}{\mu} \frac{\partial p}{\partial x} \quad (17)$$

where, sf is the surface for all fractures and γ is the matrix volume.

5. Simulation of fluid flow in NFR

Currently, there are three major approaches to simulate fluid flow through naturally fractured reservoirs which include: continuum, dual porosity/dual permeability, and flow through discrete fracture network. Recently studies revolving the use of pressure Transient data for characterizing naturally fractured reservoir through Inversion of well test data [14]. In this paper, pressure transient data from the NFR is used to evaluate the fracture map which is generated by statistical analysis of field data as per Doonechaly and Rahman [15]. This is carried out in two inversion steps.

Step 1. The reservoir is divided into a number of grid blocks and the block-based permeability tensors are estimated by considering all fractures that are intersected by the blocks. Fluid flow is simulated (forward modelling by single continuum approach, therefore the permeability tensors) to estimate change in pressure and pressure derivatives. The simulated pressure data is compared with that obtained from well test to estimate error. The gradient based technique is utilized to repeat the forward modelling for different realizations of block-based fracture permeability tensors until the error is reduced to a minimum. The optimized permeability tensors are then correlated to fracture properties of the corresponding blocks.

Step 2. In the next inversion step, different subsurface fracture maps are realized based on the correlation and the forward modelling carried out by using single continuum and discrete fracture approach, which was developed by Gholizadeh and Abdelazim *et al.* [16] until an optimized fracture map is obtained (see Fig.2 and Table.1).

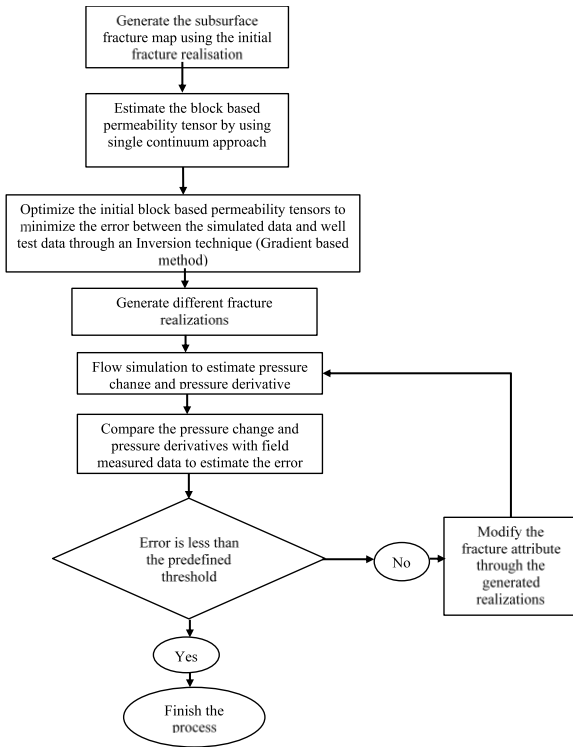


Fig. 2: The different steps used in optimizing the subsurface fracture map

Table 1. Reservoir inputs parameters for permeability tensor calculations

Parameter	Value
Reservoir dimensions	500m×500m×250m
Matrix permeability	0.0095 mD
Matrix porosity	2%
Fracture aperture	7.06×10^{-3} mm
Initial fracture intensity	0.15m^{-1}
Initial reservoir pressure	34.9 MPa, 5,063psia)
Injection pressure (injection case)	54.9 MPa, (7963.65psia)
Fluid viscosity	1.38cp
Fluid compressibility	10^{-8}MPa^{-1}
Production time before shut in (t_p)	72hrs
Production flow rate before shut in	5571bbl/d

We simulate the single-phase flow by coupling permeability tensors and flow through discrete fractures. The reservoir fracture map and grid blocks are shown in Fig. 3a, with short to medium fractures that cut these blocks. The calculated *permeability tensors* are shown in Fig. 3b.

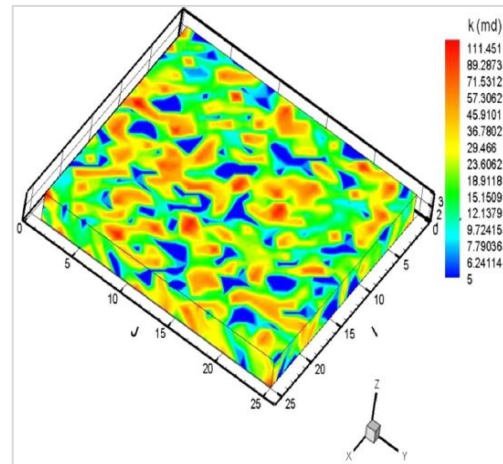
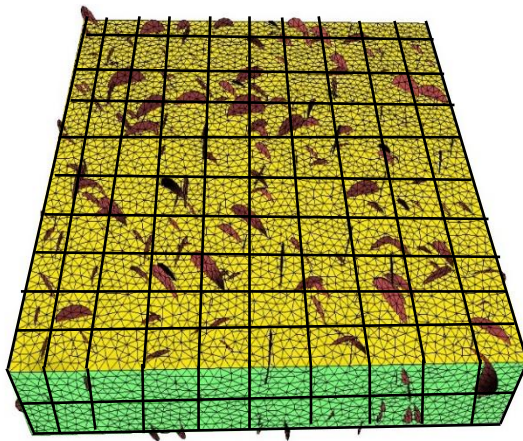


Fig. 3(a) Reservoir domain showing 3D optimized fracture map generated using the block-based permeability tensors; (b) 3D block-based permeability tensor map of the reservoir

5.1. Reservoir simulation workflow

Having optimized the fracture map, flow simulation is conducted at four different oil flow rates for 20 years (1990 – 2010): 5, 10, 15, and 20 MSTB/d. Figure 4 shows the relative permeability data used during the simulation process. Table 2 shows the calculated oil mobility

function (T_f) as a function of average reservoir pressure (p_{av}). Figure 5 shows the oil saturation changes over the simulation period. As can be seen from this figure that oil saturation changing drastically inside the fractures as the fractures considered the main source for oil in this case.

Table 2. Calculated oil mobility function data: $T_f(p_{av})$

Year	S_o	k_{ro}	p_{av} (psia)	μ_o	B_o	$T_f = k_{ro}/\mu_o B_o$
1990	0.53	0.09	5370	0.13	1.5	0.46153846
1991	0.526	0.089	2297	0.13	1.5	0.45641026
1992	0.531	0.095	2000	0.13	1.5	0.48717949
1993	0.531	0.095	1861	0.13	1.5	0.48717949
1994	0.531	0.095	1759	0.13	1.5	0.48717949
1995	0.532	0.09	1681	0.13	1.5	0.46153846
1996	0.5323	0.096	1621	0.13	1.5	0.49230769
1997	0.533	0.097	1567	0.13	1.5	0.49743590
1998	0.5328	0.0964	1518	0.13	1.5	0.49435897
1999	0.5325	0.0962	1475	0.13	1.5	0.49333333
2000	0.532	0.0957	1436	0.13	1.5	0.49076923
2001	0.531	0.0947	1398	0.13	1.5	0.48564103
2002	0.529	0.0928	1394	0.13	1.5	0.47589744
2003	0.528	0.0918	1331	0.13	1.5	0.47076923
2004	0.526	0.0899	1300	0.13	1.5	0.46102564
2005	0.524	0.0879	1271	0.13	1.5	0.45076923
2006	0.522	0.0861	1243	0.13	1.5	0.44153846
2007	0.5197	0.0838	1217	0.13	1.5	0.42974359
2008	0.518	0.0822	1193	0.13	1.5	0.42153846
2009	0.515	0.0793	1169	0.13	1.5	0.40666667
2010	0.513	0.0774	1147	0.13	1.5	0.39692308

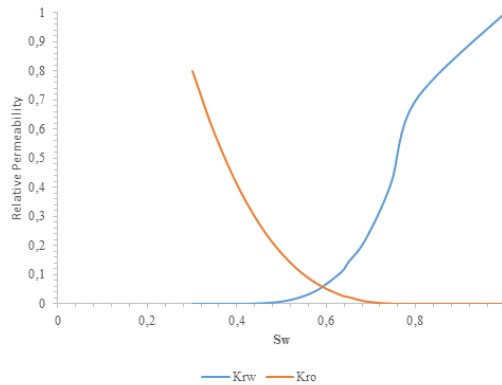


Figure 4. Relative permeability curve used in the simulation work

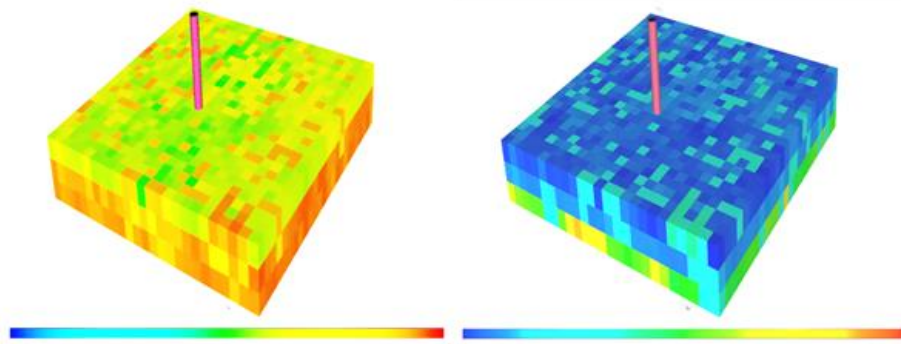


Figure 5. Reservoir simulation model. Oil saturation distribution: (a) After 4 years of oil production, and (b) after 20 years of oil production

6. Results

Data from the four different flow rate runs was combined in Table 3:

Table 3. Mobility Function (T_f) at average reservoir pressure at different flow rate

p_{av} (psia)	T_f at $q_o = 20$ STB/d	T_f at $q_o = 15$ STB/d	T_f at $q_o = 10$ STB/d	T_f at $q_o = 5$ STB/d
2297	0.4564	0.4808	0.4610	0.3772
2000	0.4872	0.4906	0.4906	0.4265
1861	0.4872	0.4906	0.4906	0.4512
1759	0.4872	0.4906	0.4901	0.4610
1681	0.4615	0.4956	0.4921	0.4660
1621	0.4923	0.4956	0.4956	0.4709
1567	0.4974	0.5005	0.4956	0.4758
1518	0.4944	0.4956	0.4956	0.4808
1475	0.4933	0.4946	0.4946	0.4857
1436	0.4908	0.4906	0.4906	0.4827
1398	0.4856	0.4857	0.4857	0.4788
1394	0.4759	0.4758	0.4758	0.4734
1331	0.4708	0.4699	0.4709	0.4660
1300	0.4610	0.4600	0.4610	0.4591
1271	0.4508	0.4497	0.4512	0.4512
1243	0.4415	0.4395	0.4413	0.4413
1217	0.4297	0.4265	0.4265	0.4314
1193	0.4215	0.4186	0.4167	0.4167
1169	0.4067	0.4068	0.4068	0.4068
1147	0.3969	0.3969	0.3969	0.4019

After collecting all data available, we plot the mobility oil function with respect of average by quadratic regression the following equation were obtained:

$$\frac{k_{rf,o}}{\mu_o \beta_o} = -2 \times 10^{-7} P_{av}^2 + 0.0007 P_{av} - 0.165 \tag{18}$$

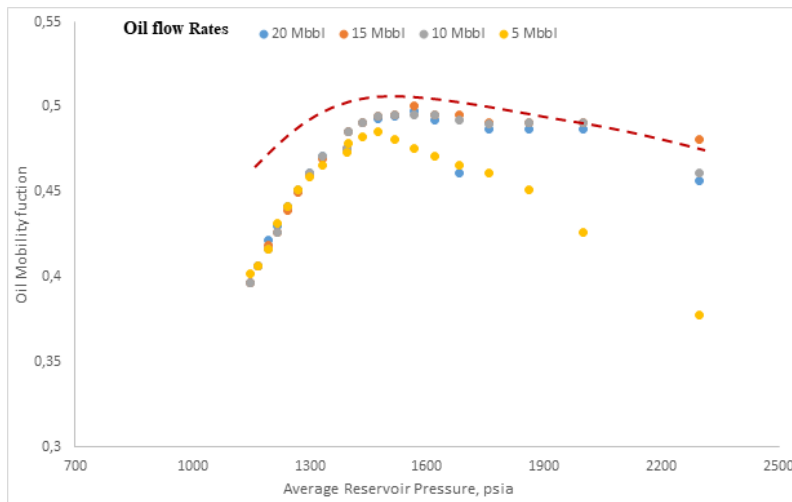


Figure 6. Oil mobility vs Average Reservoir Pressure

7. Discussions

After introducing the new mobility function to the IPR equation an IPR curve is obtained.

$$q_o = \frac{0.00708 k_f h (p_r - p_{wf})}{\left[\frac{1}{2} \ln \left(\frac{4A}{\gamma C_A r_w^2} \right) + s \right]} \left(\frac{k_{rf,o}}{\mu_o B_o} \right) p_{av} \tag{19}$$

where,

$$\frac{k_{rfo}}{\mu_o \beta_o} = -2.0 \times 10^{-7} P_{av}^2 + 0.0007 P_{av} - 0.165 \quad (20)$$

Our new correlation was compared with Vogel's and Wiggins' IPRs based on flow data used from a real well [17]. The results are shown in Fig.7. It was found that our new IPR curve gives more reliable results than the other two methods, which are not applicable to a fracture reservoir. Firstly, the well's test point data are respected by the new correlation, whereas the two other correlations significantly deviate from the test point. Secondly, the methods by Vogel and Wiggins underestimate the absolute open flow potential that a fractured reservoir (with high negative skin) can deliver.

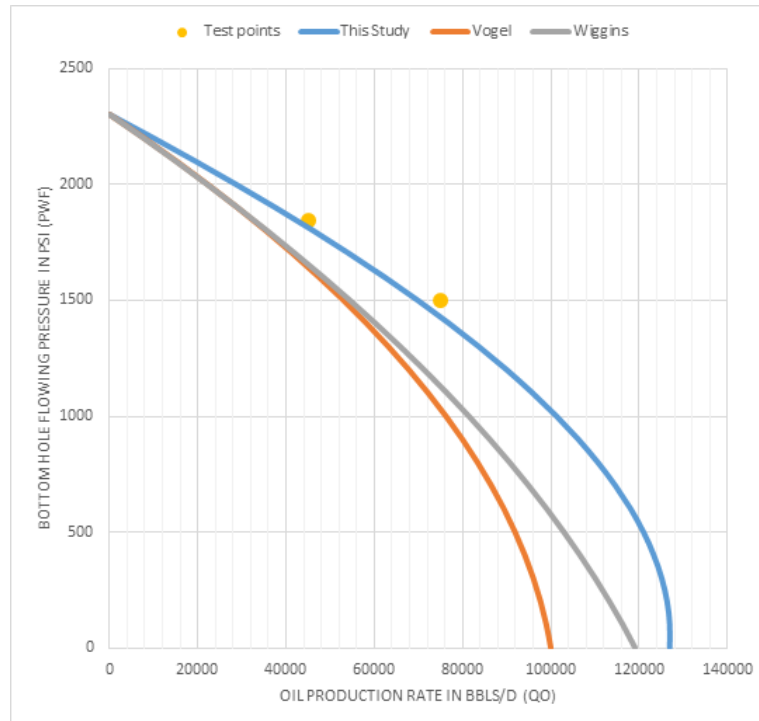


Figure 7. Inflow performance relationship curve using test well data (Jahanbani et al. [9])

8. Conclusions

The objective of this study was to develop reservoir inflow performance relationship (IPR) equation that predicts volumetric production rate as a function of average reservoir pressure in a saturated, fractured reservoir. Several IPR correlations developed in the past are not applicable for the case of a fractured reservoir.

Therefore, a new IPR equation is developed in this study based on extensive numerical reservoir simulation runs that captures fluid flow rates as a function of reservoir pressure over time.

The newly developed IPR equation is compared with two well-known IPR equations (Vogel, and Wiggins). The significant difference of oil production rate as a function of wellbore pressure underscores the fact that an IPR developed for fluid flow in non-fractured reservoir rock cannot be used for a fractured reservoir. As expected, the use of the two existing correlations for multiphase flow in fractured reservoir underestimate production rate by a wide margin.

The new IPR equation can serve as an important tool for routine reservoir flow performance by practicing engineers using a simple spreadsheet.

Nomenclature

$FBHP$	absolute open flow potential (volumetric oil flow rate at zero FBHP)
p_r	static reservoir pressure
p_{wf}	flowing bottom hole pressure (FBHP)

q	<i>volumetric oil flow rate</i>
q_{max}	<i>absolute open flow potential (volumetric oil flow rate at zero FBHP)</i>
m	<i>semi-log straight line slope, psia/cycle</i>
p	<i>pressure, psia</i>
p_{av}	<i>average pressure, psia</i>
p_i	<i>initial reservoir pressure, psia</i>
p_R	<i>average reservoir pressure, psia</i>
p_{wf}	<i>flowing wellbore pressure, psia</i>
r_e	<i>drainage radius, ft</i>
R_p	<i>cumulative produced gas/oil ratio, scf/STB</i>
R_s	<i>solution gas/oil ratio, scf/STB</i>
R_w	<i>wellbore radius, ft</i>
S	<i>skin factor</i>
S	<i>storage, ft/psia</i>
S_o	<i>oil saturation, fraction</i>
S_w	<i>water saturation, fraction</i>
t	<i>time, hours</i>
T_f	<i>fracture transmissibility, mD. Ft/cp</i>
B_g	<i>gas formation volume factor, bbl/scf</i>
B_o	<i>oil formation volume factor, bbl/STB</i>
B_t	<i>total formation volume factor, bbl/STB</i>
C_e	<i>effective compressibility, psia⁻¹</i>
C_{mt}	<i>total matrix compressibility, psia⁻¹</i>
c_o	<i>oil compressibility, psia⁻¹</i>
c_r	<i>rock compressibility, psia⁻¹</i>
c_w	<i>water compressibility, psia⁻¹</i>
h	<i>formation thickness, ft</i>
h_m	<i>matrix thickness (height), ft</i>
k_f	<i>fracture bulk permeability, md</i>
k_o	<i>effective oil permeability, md</i>
k_{ro}	<i>oil relative permeability, dimensionless</i>

References

- [1] Muskat M, and Evinger HH. Calculations of Theoretical Productivity Factor. Trans. AIME, 1942; 146: 126–139.
- [2] Vogel JV. 1968, Inflow Performance Relationships for Solution-Gas Drive Wells. J. Pet. Technol., 1968; 20(1): 83–92.
- [3] Fetkovich MJ. The Isochronal Testing of Oil Wells, Paper SPE 4529 presented at the 1973 SPE Annual Meeting, Las Vegas, Nevada, 30 September–3 October 1973.
- [4] Cheng AM. Inflow performance relationships for solution-gas-drive slanted/horizontal wells. In SPE Annual Technical Conference and Exhibition 1990. Society of Petroleum Engineers.
- [5] Wiggins ML. 1994, Generalized Inflow Performance Relationships for Three-Phase Flow. SPE Res Eng., SPE-25458-PA, 1994; 9 (3): 181-182.
- [6] Elias M, El-Banbi HA, Fattah KA and El-Tayeb ESA. New Inflow Performance Relationship for Solution-Gas Drive Oil Reservoirs. SPE/EAGE Reservoir Characterization & Simulation Conference 2009.
- [7]. Shahri MP, Shi ZR, Zhang HQ, Akbari B, Firoozabad MRM. Generalized Inflow Performance Relationship (IPR) for Horizontal Wells. In SPE Eastern Regional Meeting, Pittsburgh, PA, 2013: 20-22.
- [8] Abdelazim RA. Integration of static and dynamic reservoir data to optimize the generation of subsurface fracture map. Journal of Petroleum Exploration and Production Technology, 2016; 6(4): 691-703.
- [9] Jahanbani GA, Torsæter O and Moradi M. Inflow Performance Relationship for Horizontal Oil Wells in Fractured Reservoirs. 7th EAGE Saint Petersburg International Conference and Exhibition. November 2016.
- [10] Abdelazim R, and Rahman SS. Estimation of permeability of naturally fractured reservoirs by pressure transient analysis: An innovative reservoir characterization and flow simulation. Journal of Petroleum Science and Engineering, 2016; 145: 404-422

- [11] Abdelazim R. Prediction of Naturally Fractured Reservoir Performance using Novel Integrated Workflow. *International Journal of Advanced Computer Science and Applications*, 2017; 8(4): 115-122.
- [12] Luthi SM. Fractured reservoir analysis using modern geophysical well techniques: application to basement reservoirs in Vietnam. Geological Society, London, Special Publications, 2005; 240(1): 95-106.
- [13] Tarahhom F, Sepehrnoori K, Marcondes F. A novel approach to integrate dual porosity model and full permeability tensor representation in fractures. Paper presented at the SPE Reservoir Simulation Symposium 2009.
- [14] Morton KL, Nogueira PDB, Booth R, Kuchu, FJ. Integrated interpretation for pressure transient tests in discretely fractured reservoirs. In SPE Europec/EAGE Annual Conference. Society of Petroleum Engineers 2012.
- [15] Doonechaly NG, Rahman S. 3D hybrid tectono-stochastic modelling of naturally fractured reservoir: Application of finite element method and stochastic simulation technique. *Tectonophysics*, 2012; 541: 43-56.
- [16] Gholizadeh Doonechaly N, Abdel Azim RR, Rahman SS (2016). A study of permeability changes due to cold fluid circulation in fractured geothermal reservoirs. *Groundwater*, 2016; 54(3): 325-335.
- [17] Janban, A, Shadizadeh SR. Determination of the Inflow Performance Relationship in Naturally Fractured Oil Reservoirs: Analytical Considerations. *Energy Sources, Part A: Recovery, Utilization, and Environmental Effects*, 2013; 35(8): 762-777.

To whom correspondence should be addressed: Assoc. prof. Reda Abdel Azim, American University of Ras Al Khaimah, United Arab Emirates, Ras Al Khaimah, Reda.abdelazim@aurak.ac.ae